Revista Brasileira de Ciências Ambientais
Brazilian Journal of Environmental Sciences

Satellite images for rainfall estimation in Espírito Santo State, Brazil

Imagens de satélite para a estimativa de precipitação no estado do Espírito Santo, Brasil

Lucas Silveira Fuentes[1], *José Antonio Tosta dos Reis*[1], *Antônio Sérgio Ferreira Mendonça*[1], *Fernando das Graças Braga da Silva*[2], *Matheus David Guimarães Barbedo*[2]

ABSTRACT

Due to the inadequate distribution, scarcity, or operational problems of rain gauges or pluviographs, remote sensing has been considered a relevant alternative for characterizing the regime and measuring the rainfall intensities. The present paper evaluated estimates of annual precipitation totals in the state of Espírito Santo, Brazil, established from conventional monitoring conducted by rain gauges and the manipulation of satellite images. Additionally, it assessed the quality of estimates during El Niño and La Niña years. For the study, the 3B42 version seven products from the Tropical Rainfall Measuring Mission (TRMM) satellite and the 3IMERGDF version six products from the Global Precipitation Measurement (GPM) satellite were used. These satellites were developed through a partnership between the National Aeronautics and Space Administration and the Japan Aerospace Exploration Agency. Historical series from the years 2001–2019 of 83 rain gauge stations installed and operating in the state of Espírito Santo and its surroundings were analyzed, along with satellite images from TRMM and GPM for spatial grids of 25 and 10 km, respectively. The parameters recommended by the International Precipitation Working Group were used to conduct the analysis. The TRMM satellite performed better during La Niña periods (R^2=0.941; root mean square error [RMSE]=44.21 mm; ME=14.87 mm), surpassing the results observed in El Niño (R^2=0.885; RMSE=141.5 mm; ME=−87.14 mm). Although the GPM satellite performed stably between El Niño and La Niña periods, with systematic underestimation (bias≈0.93) and similar ME (ME≈79 mm), it showed a lower correlation with rain gauge records (R^2≈0.77) than the TRMM satellite. The results indicated that the use of satellite images was a consistent alternative for the appropriation of annual precipitation totals and that the TRMM satellite presented more accurate estimates, both for long-term analysis and for the El Niño and La Niña periods.

Keywords: tropical rainfall measuring mission; global precipitation measurement; rain gauges; remote sensing.

RESUMO

Em função da inadequada distribuição, da escassez ou de problemas na operação de estações pluviométricas, o uso do sensoriamento remoto tem sido considerado relevante alternativa para a caracterização do regime de chuvas e a apropriação de intensidades precipitadas. O presente trabalho avaliou estimativas de totais anuais precipitados no estado do Espírito Santo, Brasil, estabelecidas por meio do monitoramento convencional conduzido por pluviômetros e da manipulação de imagens de satélites. Adicionalmente, avaliou a qualidade das referidas estimativas em anos de El Niño e La Niña. Para a condução do estudo foram utilizados os produtos 3B42, versão 7, do satélite Tropical Rainfall Measuring Mission (TRMM) e 3IMERGDF, versão 6, do satélite Global Precipitation Measurement (GPM), satélites desenvolvidos por meio de uma parceria entre a National Aeronautics and Space Administration (NASA) e a Agência Japonesa de Exploração Aeroespacial (JAXA). Foram analisadas séries históricas entre os anos de 2001 e 2019 de 83 postos pluviométricos instalados e em operação no estado do Espírito Santo e entorno, além de imagens orbitais dos satélites TRMM e GPM para malhas espaciais de 25 e 10 km, respectivamente. Para a condução da análise foram utilizados os parâmetros recomendados pelo International Precipitation Working Group (IPWG). O satélite TRMM apresentou melhor desempenho durante os períodos de La Niña (R^2=0,941; RMSE=44,21 mm; mean error [ME]=14,87 mm), superando os resultados observados em El Niño (R^2=0,885; RMSE=141,5 mm; ME=−87,14 mm). Ainda que o satélite GPM tenha desempenho estável entre os períodos de El Niño e La Niña, com subestimação sistemática (bias≈0,93) e erro médio semelhante (ME≈79 mm), apresentou menor correlação com os registros de pluviômetros (R^2≈0,77) que o satélite TRMM. Os resultados demonstraram que a utilização das imagens de satélite se apresentou como alternativa consistente para a apropriação de totais anuais precipitados e que o satélite TRMM apresentou estimativas mais precisas, tanto para a análise de longo período quanto para os períodos de El Niño e La Niña.

Palavras-chave: *tropical rainfall measuring mission*; *global precipitation measurement*; pluviômetros; sensoriamento remoto.

[1]Universidade Federal do Espírito Santo – Vitória (ES), Brazil.

[2]Universidade Federal de Itajubá – Itajubá (MG), Brazil.

Corresponding author: José Antonio Tosta dos Reis – Avenida Fernando Ferrari, 514 – Campus Universitário de Goiabeiras – CEP: 29075-910 – Vitória (ES), Brazil. E-mail: jatreis@gmail.com

Conflicts of interest: the authors declare no conflicts of interest.

Funding: none.

Received on: 08/07/2024. Accepted on: 06/24/2025.

https://doi.org/10.5327/Z2176-94782228

Introduction

Precipitation monitoring is essential for various fields, such as agriculture, water resource management, and the forecasting of extreme weather events. There are different ways to measure precipitation, with rain gauges being the oldest and most widely used instruments since the 19th century. These devices are installed on the ground and measure the amount of water that falls directly onto their collection surfaces. A more recent alternative is the use of satellites, which are capable of estimating precipitation through atmospheric observations. Satellites offer broad coverage and provide data regularly, making them an important tool for monitoring rainfall conditions (Huffman et al., 2007).

The integration of information from different sources, in addition to increasing the reliability of records, can enhance the accuracy of precipitation estimates in regions where data from a single source proves insufficient. This approach is relevant for assessing data quality and identifying possible limitations and inconsistencies associated with each source (Adler et al., 2003; Fan et al., 2021; Guo et al., 2024).

The use of satellites has gained importance for monitoring precipitation in remote regions, where the availability of rain gauges is limited and data collection is performed irregularly (Macharia et al., 2020; Sharma et al., 2020; Mekonnen et al., 2021). Satellite-based precipitation monitoring, due to its broad spatial coverage, has become increasingly common in response to the effects of climate change, particularly changes in the intensity and frequency of El Niño and La Niña events (Pedreira Junior et al., 2020; Mokhov, 2022; Wu, 2024). It is important to note that El Niño and La Niña phenomena can lead to more severe droughts or more intense rainfall in different regions of the globe, causing environmental disasters and compromising ecosystem balance, food production, and the integrity of urban environments (Li et al., 2019; Silva et al., 2020; Haines and Lam, 2023; Lal and Singh, 2023; Lee et al., 2023).

Among the most frequently used satellites for precipitation monitoring are the Tropical Rainfall Measurement Mission (TRMM) and the Global Precipitation Measurement Mission (GPM).

The TRMM satellite was developed through a collaboration between the National Aeronautics and Space Administration (NASA) and the Japan Aerospace Exploration Agency (JAXA), launched in November 1997, and decommissioned in June 2015. The primary focus of TRMM was to collect accurate and detailed precipitation measurements, providing a deeper understanding of rainfall patterns in the tropical regions of the globe (Kummerow et al., 2000). The satellite was equipped with a set of instruments, including a microwave radiometer and a precipitation radar, which enabled the collection of data on the amount and intensity of precipitation on a global scale, with daily temporal resolution and a spatial resolution of 25 km².

The TRMM mission was essential for enhancing the understanding of climatic processes in tropical regions and improving the forecasting of extreme weather events, such as floods and droughts. Its data contributed significantly to the improvement of weather prediction models and to a better understanding of the interactions between the atmosphere and the oceans in these regions, as demonstrated in the studies by Almeida et al. (2020), Chen et al. (2020), Montazeri et al. (2020), Raj et al. (2021), Suroso et al. (2023), and Tunas et al. (2024).

The GPM satellite, the result of a global partnership among various space agencies, was launched in February 2014. GPM is an evolution of the TRMM mission, featuring significant improvements in global coverage and precipitation measurement technology. The satellite is equipped with a series of advanced instruments designed to measure precipitation with high accuracy and detail. The core instrument of GPM is the dual-frequency precipitation radar (DPR), which uses two types of microwave frequencies to detect precipitation and estimate the amount of rainfall and snowfall. The DPR provides information on cloud vertical structure and precipitation intensity, enabling a deeper understanding of atmospheric processes. Its temporal resolution is daily, and its spatial resolution is 10 km². Applications using imagery generated by GPM are found in studies by Kukulies et al. (2020), Nan et al. (2021), Fan et al. (2023), and Woods et al. (2023).

In addition to monitoring alternatives, other relevant issues concerning the precipitation regime in Brazil are the variations resulting from the El Niño-Southern Oscillation (ENSO) cycle, which arises from the coupling between the ocean and the atmosphere through anomalies in sea surface temperature in the equatorial Pacific Ocean and anomalies in atmospheric pressure. ENSO has an oceanic component called El Niño (associated with abnormal warming of the Pacific Ocean waters) or La Niña (resulting from abnormal cooling of the Pacific Ocean). The Southern Oscillation, in turn, constitutes the atmospheric component of ENSO (Reboita et al., 2021).

During El Niño events, negative precipitation anomalies are recorded in the North and Northeast regions of Brazil, while the South region generally exhibits positive anomalies. This pattern tends to reverse in years influenced by the La Niña phenomenon (Cai et al., 2020; Medeiros et al., 2020; Reboita et al., 2021; Santos et al., 2023). In the Southeast region of Brazil, the low consistency of anomalies associated with ENSO is due to the transitional nature of the area (Duarte and Ribeiro, 2023).

The state of Espírito Santo, located in the Southeast region of Brazil, is frequently affected by extreme hydrological events, such as droughts and floods, and was defined as the study area for this research. In this context, the use of satellite imagery as an alternative or complementary source to conventional rain gauge data proves to be a valuable tool for estimating and analyzing the spatial distribution of precipitation, especially in regions with low meteorological station density.

Based on the combination of image processing techniques and statistical analysis, this study aimed to evaluate precipitation estimates obtained through remote sensing from the TRMM and GPM satellites in relation to conventional rain gauge records, also considering the influence of El Niño and La Niña phenomena on the rainfall regime.

Materials and Methods

Study area

The state of Espírito Santo is located in the Southeast region of Brazil. The state features a varied tropical climate, with coastal areas characterized by well-distributed rainfall and higher regions experiencing milder temperatures. Its relief is marked by diversity, ranging from coastal plains to mountains. Regarding land use, the coast is occupied by cities, industries, and agricultural activities, while the interior encompasses forested and agricultural areas. The economy is diverse, with a strong emphasis on the steel industry. Additionally, agriculture and livestock, fishing, and tourism are also important economic pillars in the region (IPEA, 2021).

Two different evaluations were conducted in this research. The first evaluation aimed to compare annual total precipitation records obtained from rain gauge operations with annual totals estimated from images produced by the TRMM and GPM satellites. A second evaluation performed a similar comparison, considering a partial series of annual total precipitation recorded during El Niño and La Niña years. Figures 1 and 2 present flowcharts summarizing the different activities carried out in these evaluations.

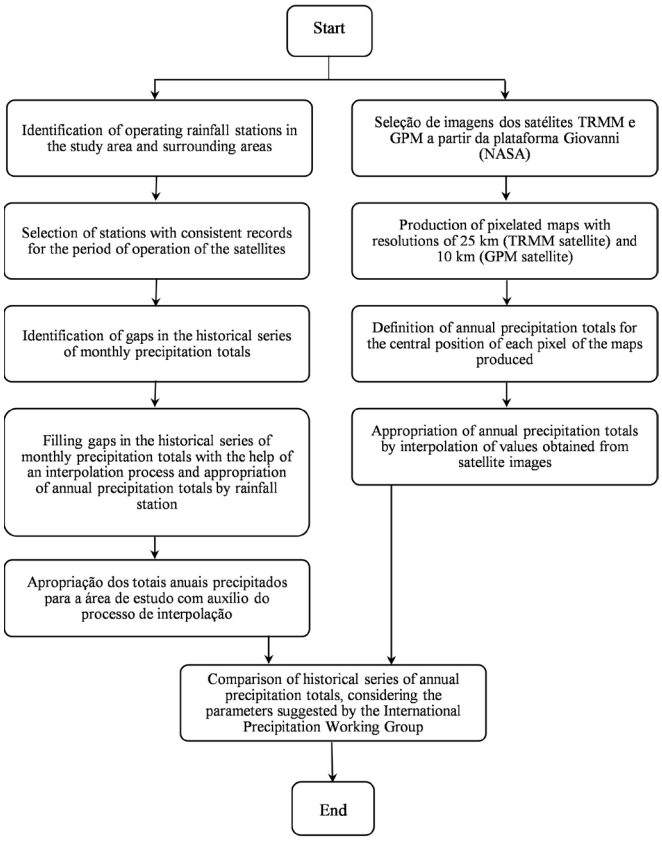

Figure 1 – Flowchart of activities for comparing annual total precipitation records obtained from rain gauges and estimated from satellite images.

Conventional rain gauge records

Rain gauge stations were selected from the hydrological data portal (Hidroweb) of the National Water and Basic Sanitation Agency (ANA), considering exclusively stations with consistent data during a period overlapping the operational period of the satellites (the period between 2001 and 2019). To increase the consistency of the interpolation process associated with the estimation of total precipitation, stations installed and operating in the surroundings of the state of Espírito Santo were also considered, including stations in operation in the states of Minas Gerais and Rio de Janeiro.

In this context, 83 (eighty-three) rain gauge stations were selected, listed in Table 1 and spatially distributed as shown in Figure 3.

Using the historical series from the selected rain gauge stations, gaps in the annual total precipitation data were filled through interpolation of the monthly total precipitation records. This gap-filling process was conducted using inverse distance weighted (IDW) interpolation and executed with the QGIS software. As described by Silva et al. (2019), the IDW method is a deterministic interpolation technique that estimates the values of a variable of interest—in this study, annual total precipitation—at unsampled locations based on a weighted average of observed values. The weights assigned to sampled points are inversely proportional to the distance to the estimation point, so that the greater the distance, the less influence the point has on the interpolation.

After filling the gaps, maps of annual total precipitation were produced for each year of the analyzed historical series. Subsequently, through georeferenced image files (raster files) of the annual total precipitation, it was possible to obtain an average annual total precipitation value for the state of Espírito Santo for each year of the historical series.

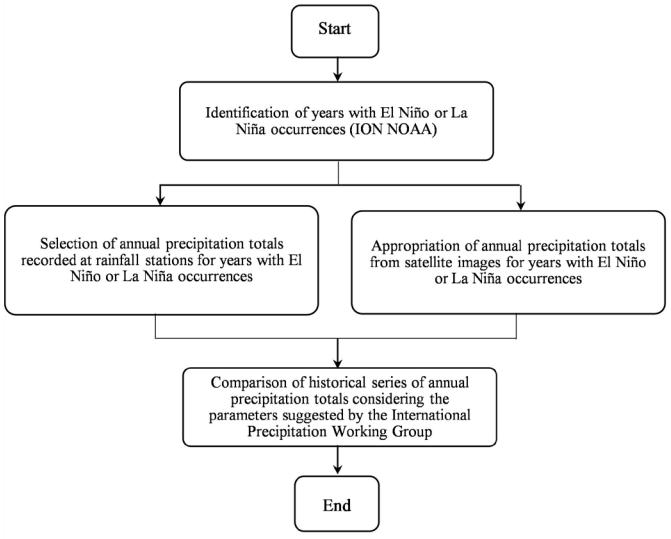

Figure 2 – Flowchart of activities for comparing annual total precipitation records obtained from rain gauges and estimated from satellite images, considering partial series for El Niño and La Niña years.

Table 1 – Selected rain gauge stations.

Identification	Code (ANA)	Watershed	Identification	Code (ANA)	Watershed
01	1840017	Itaúnas	43	1940021	Piraque-acu
02	1840012	Itaúnas	44	2040003	Santa Maria
03	1839000	Itaúnas	45	2040014	Santa Maria
04	1839001	Itaúnas	46	2040010	Santa Maria
05	1840003	Itaúnas	47	2040008	Santa Maria
06	1840004	São Mateus	48	2040018	Santa Maria
07	1840007	São Mateus	49	2040007	Santa Maria
08	1840009	São Mateus	50	2040035	Jucu
09	1840010	São Mateus	51	2040012	Jucu
10	1840013	São Mateus	52	2041020	Jucu
11	1840015	São Mateus	53	2040023	Jucu
12	1840016	São Mateus	54	2040001	Jucu
13	1840019	São Mateus	55	2040045	Jucu
14	1841006	São Mateus	56	2040004	Benevente
15	1841007	São Mateus	57	2040011	Benevente
16	1841008	São Mateus	58	2040020	Benevente
17	1841009	São Mateus	59	2040009	Benevente
18	1841010	São Mateus	60	2040005	Benevente
19	1841018	São Mateus	61	2040017	Benevente
20	1841021	São Mateus	62	2041017	Itapemirim
21	1840020	São Mateus	63	2041013	Itapemirim
22	1840026	São Mateus	64	2041018	Itapemirim
23	1839006	Doce	65	2041011	Itapemirim
24	1939002	Doce	66	2041016	Itapemirim
25	1940016	Doce	67	2041019	Itapemirim
26	1840000	Doce	68	2041003	Itapemirim
27	1940000	Doce	69	2041021	Itapemirim
28	1940009	Doce	70	2041002	Itapemirim
29	1940012	Doce	71	2041010	Itapemirim
30	1941003	Doce	72	2041015	Itapemirim
31	1941008	Doce	73	2041000	Itapemirim
32	1941009	Doce	74	2040006	Itapemirim
33	1941012	Doce	75	2140000	Itapemirim
34	1940005	Doce	76	2041005	Itabapoana
35	1940006	Doce	77	2041014	Itabapoana
36	1940013	Doce	78	2041046	Itabapoana
37	1940023	Doce	79	2141014	Itabapoana
38	2041023	Doce	80	2141015	Itabapoana
39	1940010	Piraque-acu	81	2141016	Itabapoana
40	1940002	Piraque-acu	82	2141017	Itabapoana
41	1940003	Piraque-acu	83	2041001	Itabapoana
42	1940007	Piraque-acu			

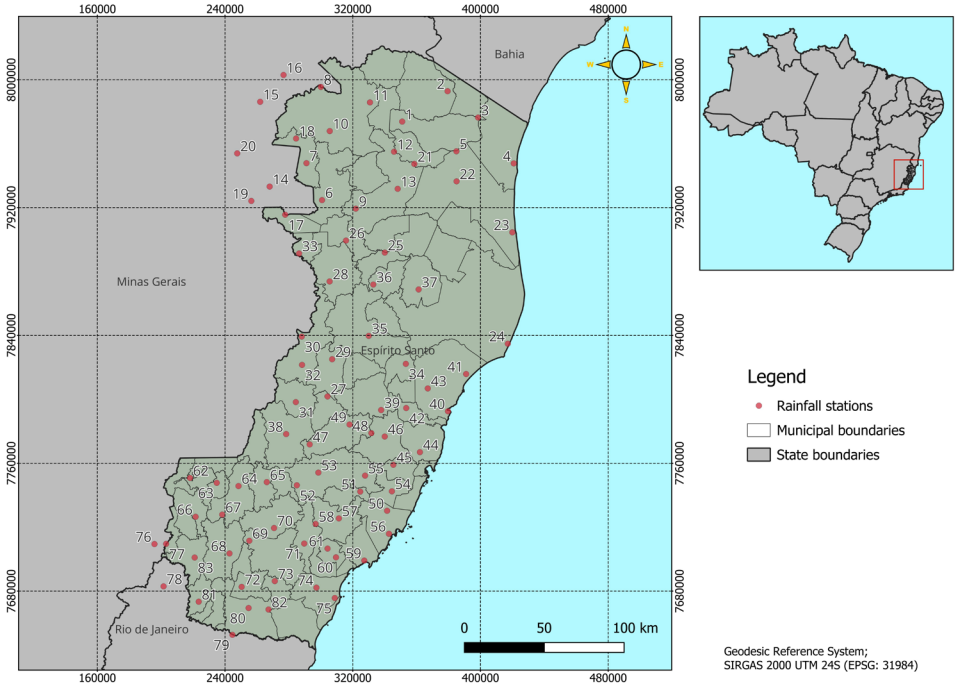

Figure 3 – Spatial location of the selected rain gauge stations.

Precipitation estimates by remote sensing

The data used in this study were obtained from the Giovanni platform (Goddard Interactive Online Visualization ANd aNalysis Infrastructure), developed and managed by the NASA. The products selected were 3B42 (version 7) from the TRMM satellite and 3IMERGDF (version 6) from the GPM satellite, corresponding to the state of Espírito Santo for the period from 2001 to 2019. Based on the selected area and time interval, 19 raster files corresponding to the annual total precipitation were generated for each satellite.

Subsequently, pixelated maps with different resolutions were generated, since the TRMM satellite produces images with a resolution of 25 km×25 km, and the GPM satellite produces images with a resolution of 10 km×10 km. To standardize the formatting of the maps from all sources (rain gauges, TRMM satellite, and GPM satellite), points were generated at the center of each pixel in the raster files corresponding to the satellite images. From these generated points, an interpolation process similar to that employed for the rain gauge data was conducted. This stage of the work was also carried out with the aid of QGIS software.

Identification of years with the occurrence of El Niño or La Niña

The comparison between annual total precipitation recorded by rain gauges and annual totals estimated from images produced by the TRMM and GPM satellites during El Niño and La Niña years involved the use of an index representing the average Pacific Ocean temperature by quarter (Oceanic Niño Index, ONI), established by the National Oceanic and Atmospheric Administration, following the approach used by Glantz and Ramirez (2020) and Bunde et al. (2024).

According to the Center for Weather Forecasting and Climate Studies (CPTEC, 2023) of the National Institute for Space Research, a year is classified as El Niño if the ONI reaches a minimum of 0.5 for at least five consecutive quarters; for La Niña, the ONI must reach a maximum of -0.5. Based on this criterion, El Niño and La Niña years were identified, as summarized in Table 2.

Subsequently, for the subset of years with the occurrence of El Niño and La Niña, a comparative analysis similar to that conducted for the originally analyzed set of rainfall records was performed.

It is important to note that segmenting the analysis based on the phases of the ENSO phenomenon made it possible to investigate the performance of TRMM and GPM satellite products under different climatic conditions associated with El Niño and La Niña events. This approach, still uncommon in regional studies in Brazil, expands the understanding of precipitation estimate behavior in specific climatic contexts.

Performance analysis

For the comparative analysis of precipitation data, four statistical parameters suggested by the International Precipitation Working Group were used—bias (Equation 1), ME (Equation 2), root mean square error (RMSE, Equation 3), and the coefficient of determination (R^2, Equation 4)—as detailed and discussed by Almeida et al. (2020).

Table 2 – El Niño and La Niña Years.

El Niño	2002
	2004
	2009
	2015
	2019
La Niña	2007
	2008
	2010
	2011
	2016

$$BIAS = \frac{\left(\frac{\sum_{i=1}^{n} Z}{n}\right)}{\left(\frac{\sum_{i=1}^{n} P}{n}\right)} \quad (1)$$

$$EM = \frac{\sum_{i=1}^{n} (P - Z)}{n} \quad (2)$$

$$RMSE = \sqrt{\frac{\sum_{i=1}^{n} (P - Z)^2}{n}} \quad (3)$$

$$R^2 = \left(\frac{\sum_{i=1}^{n} (P - \overline{P}).(Z - \overline{Z})}{\sqrt{\sum_{i=1}^{n} (P - \overline{P})^2 . (Z - \overline{Z})^2}}\right) \quad (4)$$

In Equations 1 to 4:
P: Annual total precipitation recorded by rain gauges;
Z: Annual total precipitation estimated by remote sensing;
$\overline{P}$: Mean of the annual total precipitation data recorded by rain gauges;
$\overline{Z}$: Mean of the annual total precipitation data estimated by remote sensing;
N: Number of years analyzed.

Results and Discussion

Annual total precipitation maps were produced for each year of the analyzed period (from 2001 to 2019), based on the different sources of precipitation records. Figure 4 presents maps generated from the various sources of precipitation data for the year 2008, a year marked by the occurrence of La Niña. Figure 5, in turn, shows maps generated from the different data sources for the year 2015, during an El Niño event. Similar maps were produced for all other years of the historical series analyzed.

From the mentioned maps, the average annual total precipitation was extracted for each year of the analyzed historical series for the state of Espírito Santo. The results of this stage, by source of precipitation records, are summarized in Table 3.

From the analysis of the historical series compiled in Table 3, taking as a reference the historical series established from rain gauge operations, the statistical parameters summarized in Table 4 were obtained.

The analysis of the results summarized in Table 4 shows that the lowest ME and RMSE, as well as the highest coefficient of determination (R^2), were obtained from the precipitation records derived from the TRMM satellite. This condition indicates a closer agreement with precipitation values measured by rain gauges. The obtained coefficient of determination (R^2=0.92) was considered satisfactory and is consistent with results reported by Almeida et al. (2020) in the Itapemirim River basin (Espírito Santo, Brazil); Collischonn et al. (2007) in the São Francisco River basin (Brazil); Louzada et al. (2018) in the Doce River basin (Brazil); and Yang et al. (2018) in the Dadu River basin (China).

On the other hand, in regions located outside the tropical zone, data from the GPM satellite showed superior performance compared to TRMM. Zhang (2018) identified greater accuracy in precipitation estimates obtained by GPM in a study area located in China, outside the tropical belt. Similar results were reported by Ma et al. (2016), who evaluated GPM data referring to the summer of 2014 on the Tibetan Plateau, especially at altitudes above 4,200 m. Although with relatively modest performance, Retalis et al. (2020) also indicated better results when handling GPM satellite imagery in the evaluation of annual total precipitation on the island of Cyprus. Similarly, Zhao et al. (2023), studying the Heihe River basin in China, reported that GPM showed better correlation with field data and lower root mean square error compared to TRMM; however, they noted that both satellites underestimated precipitation, especially during winter. Almazroui and Islam (2023), in turn, indicated that GPM outperformed TRMM in monthly precipitation estimates in Saudi Arabia, although both underestimated low precipitation events.

It is also important to note that the negative value associated with the ME and a bias value greater than one indicate that the annual total precipitation derived from the TRMM satellite images was moderately overestimated, a condition similar to that observed in the results produced by Almeida et al. (2020) during the evaluation of precipitation in the Itapemirim River basin (Espírito Santo, Brazil). Conversely, the annual total precipitation estimated from the GPM satellite images showed the opposite behavior, a condition also observed by Tan and Duan (2017) when processing GPM satellite images for the Singapore region.

The analysis of precipitation records during El Niño periods (2002, 2004, 2009, 2015, and 2019) and La Niña periods (2007, 2008, 2010, 2011, and 2016) involved handling different subsets of years from the originally analyzed historical series, grouped as previously indicated in Table 2. The statistical parameters (bias, ME, RMSE, and R^2) associated with the historical series produced from the processing of TRMM and GPM satellite images are summarized in Table 5.

The evaluation of the statistical parameters summarized in Table 5 reveals important aspects related to the performance of the TRMM and GPM satellites during El Niño and La Niña events. Precipitation estimates derived from GPM satellite images maintained stable values of ME and coefficient of determination (R^2) between the two analyzed periods, suggesting that the quality of the estimates was not significantly affected by climatic variations associated with the ENSO phenomenon.

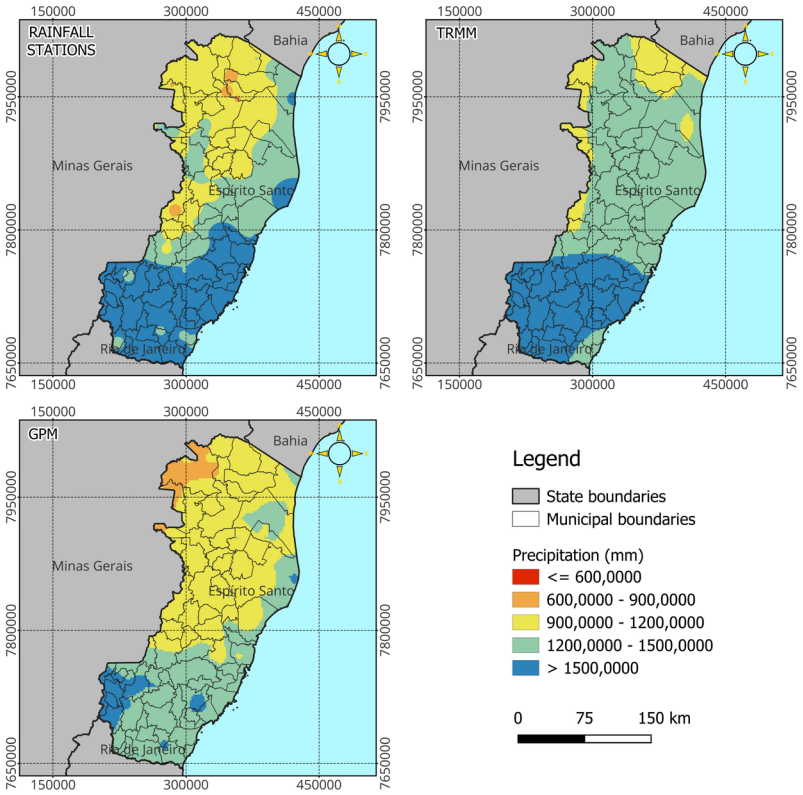

Figure 4 – Maps of annual total precipitation for the year 2008, a La Niña period, based on different sources of precipitation records.

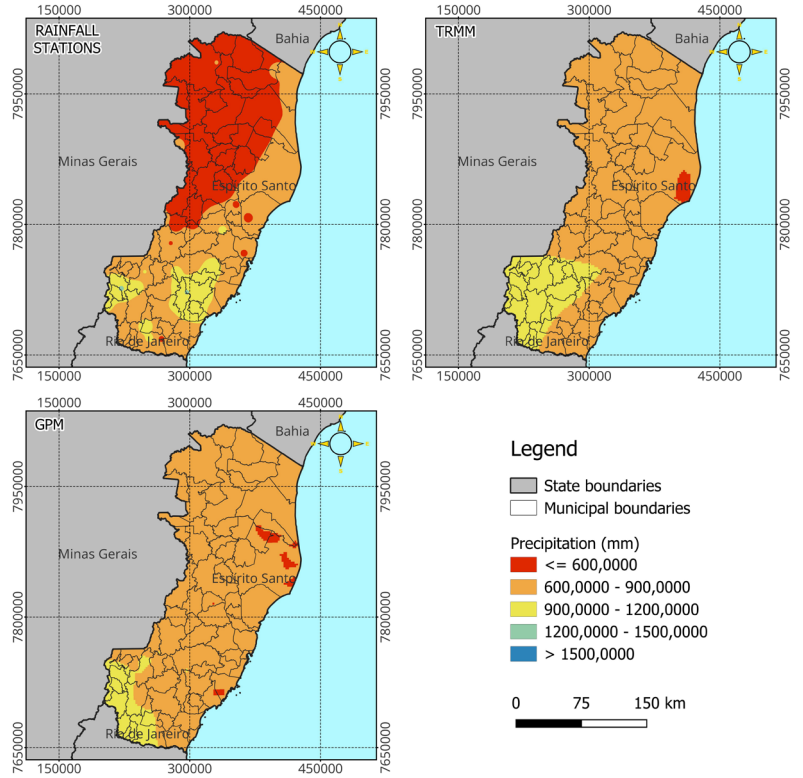

Figure 5 – Maps of annual total precipitation for the year 2015, an El Niño period, based on different sources of precipitation records.

Table 3 – Estimated annual totals (mm) for the state of Espírito Santo.

Year	Rain gauges	TRMM	GPM
2001	1,208.8	1,320.2	1,098.3
2002	1,199.5	1,332.6	1,297.9
2003	1,006.0	1,078.8	1,185.2
2004	1,565.1	1,699.2	1,529.6
2005	1,712.0	1,736.1	1,253.7
2006	1,377.9	1,418.6	1,301.5
2007	943.2	919.5	864.3
2008	1,372.2	1,382.0	1,184.2
2009	1,500.9	1,379.6	1,201.5
2010	1,181.8	1,216.2	1,028.4
2011	1,334.0	1,245.2	1,398.8
2012	1,081.8	1,101.7	1,041.3
2013	1,529.8	1,508.4	1,370.6
2014	912.5	933.7	817.2
2015	673.8	756.5	737.3
2016	1,010.4	1,004.3	968.2
2017	1,015.3	1,064.9	711.9
2018	1,436.0	1,531.6	1,383.9
2019	1,000.1	1,207.2	776.4

Table 4 – Statistical parameters derived from precipitation data for the period between 2001 and 2019.

Satellite	Bias	Mean error	RMSE	R^2
TRMM	1.034	-40.81	86.68	0.916
GPM	0.917	100.58	180.17	0.685

Table 5 – Statistical Parameters for the El Niño and La Niña Periods.

Period	Satellite	Bias	Mean error	RMSE	R^2
El Niño	TRMM	1.073	-87.14	141.5	0.885
	GPM	0.933	79.37	175.89	0.775
La Niña	TRMM	0.987	14.87	44.21	0.941
	GPM	0.932	79.53	119.22	0.774

Although the stability of these parameters indicates consistency, it is important to highlight that the performance observed specifically during El Niño and La Niña periods was superior to that observed when considering the entire historical series.

The values of bias and ME, on the other hand, suggest that the GPM satellite exhibited a persistent pattern of underestimating total precipitation across all evaluated periods. This behavior indicates a systematic tendency to produce values lower than those observed, regardless of the variations imposed by the ENSO cycle.

Precipitation estimates derived from TRMM satellite images showed greater sensitivity to climatic fluctuations associated with El Niño and La Niña. The increase in R^2 values, accompanied by reductions in ME and RMSE during La Niña years, indicates that estimates made in this period performed substantially better compared to those obtained during El Niño years.

It is important to note that the overestimation of precipitation values from TRMM satellite images during El Niño years (also observed when analyzing the entire historical series), as evidenced by bias and ME, shifted to a moderate underestimation during La Niña years. Additionally, the increase in R^2 and the reduction in RMSE indicate that the processing of TRMM satellite images yielded better results during the La Niña period than during the El Niño period.

The assessment of precipitation behavior during El Niño and La Niña periods based on satellite image observations has also been the focus of various studies conducted in different climatic contexts. Koralegedara et al. (2023) investigated the interannual variability of daytime precipitation during the boreal spring (March and April) in Sri Lanka, the second-largest island in the Indian Ocean. The main focus was to understand how ENSO events modulate this variability. The analysis was based on precipitation estimates from the GPM and TRMM satellites, covering the period from 2001 to 2019. The study concluded that ENSO events have a significant influence on daytime precipitation during spring in Sri Lanka. Specifically, La Niña events are associated with an intensification of daytime precipitation, while El Niño events tend to substantially reduce precipitation.

Chavda et al. (2024) analyzed precipitation regimes in California between 2001 and 2019. The study involved processing GPM satellite data, as well as precipitation records from the Global Precipitation Climatology Centre as ground reference. According to the authors, the analysis revealed that, contrary to what was believed before 2000, El Niño had a significant negative correlation with precipitation in southern California, indicating lower rainfall volumes during El Niño months. Both satellite and ground data confirmed this trend, highlighting changes in regional climate patterns over the past two decades.

Restrepo-Coupe et al. (2024), in turn, investigated the impacts of extreme El Niño (2015–2016) and La Niña (2008–2009) events on the Tapajós National Forest (Brazil), combining over two decades of observations using eddy covariance (a micrometeorological technique that measures the exchange of gases, water vapor, and energy between the land surface and the atmosphere) with monthly precipitation data obtained from the GPM and TRMM satellites. Satellite images were used to monitor climate variability and precipitation patterns associated with ENSO, allowing characterization of the forest's responses to drought and excessive moisture. According to the authors, during La Niña, there was a net carbon loss due to reduced photosynthesis caused by lower solar radiation, even without an increase in ecosystem respiration. Conversely, the El Niño period caused intense drought, resulting in temporary carbon gains due to strong suppression of respiration, an effect that

lasted more than 3 years. The study concludes that the Amazon forest is more sensitive to drought than to excess rainfall, with drought being a significant degradation factor in the face of future climate change.

Conclusions

The statistical analysis performed demonstrated that precipitation data obtained via remote sensing satisfactorily reproduced field records from rain gauges. Although the TRMM satellite represents an earlier technology, it provided more consistent precipitation estimates for the state of Espírito Santo compared to the GPM satellite. This higher accuracy can be attributed to the fact that TRMM was developed for monitoring tropical regions, which characterizes the study area.

The TRMM satellite showed superior performance during La Niña periods. The GPM satellite, in turn, demonstrated more stable performance throughout the historical series, with similar results in both El Niño and La Niña periods.

The results obtained highlighted the effectiveness of using remote sensing data for monitoring precipitation regimes in different climatic contexts.

Authors' Contributions

Fuentes, L.S.: Conceptualization; Data Curation; Investigation; Methodology; Software; Validation; Visualization; Writing – Original Draft; Writing – Review and Editing. **Reis**, J.A.T.: Conceptualization; Methodology; Supervision; Validation; Visualization; Writing – Original Draft; Writing – Review and Editing. **Mendonça**, A.S.F.: Validation; Visualization; Writing – Original Draft; Writing – Review and Editing. **Silva**, F.G.B.: Validation; Visualization; Writing – Original Draft; Writing – Review and Editing. **Barbedo**, M.D.G.: Validation; Visualization; Writing – Original Draft; Writing – Review and Editing.

References

Adler, R.F.; Huffman, G.J.; Chang, A.; Ferraro, R.; Xie, P.P.; Janowiak, J.; Schneider, U.; Curtis, S.; Bolvin, D.; Gruber, A.; Susskind, J.; Arkin, P.; Nelkin, E., 2003. The Version-2 Global Precipitation Climatology Project (GPCP) monthly precipitation analysis. Journal of Hydrometeorology, v. 4 (6), 1147-1167. https://doi.org/10.1175/1525-7541(2003)004<1147:TVGPCP>2.0.CO;2

Almazroui, M.; Islam, M.N., 2023. Spatiotemporal evaluation of five satellite-based precipitation products under the arid environment of Saudi Arabia. AIP Advances, v. 13 (4), 045222. https://doi.org/10.1063/5.0191924

Almeida, K.N.; Reis, J.A.T.; Buarque, B.C.; Mendonca, A.S.F.; Rodrigues, M.B.; Sa, G.L.N., 2020. Performance analysis of TRMM satellite in precipitation estimation for the Itapemirim River basin, Espirito Santo state, Brazil. Theoretical and Applied Climatology, v. 141, 791-802. https://doi.org/10.1007/s00704-020-03204-5

Bunde, A.; Ludescher, J.; Schellnhuber, H.J., 2024. Evaluation of the real-time El Niño forecasts by the climate network approach between 2011 and present. Theoretical and Applied Climatology, v. 155, 6727-6736. https://doi.org/10.1007/s00704-024-05035-0

Cai, W.; McPhaden, M.J.; Grimm, A.M.; Rodrigues, R.R.; Taschetto, A.S.; Garreaud, R.D.; Dewitte, B.; Poveda, G.; Ham, Y.-G.; Santoso, A.; Ng, B.; Anderson, W.; Wang, G.; Geng, T.; Jo, H.S.; Marengo, J.; Alves, L. M.; Osman, M.; Li, S.; Wu, L.; Karamperidou, C.; Takahashi, K.; Vera, C., 2020. Climate impacts of the El Niño-Southern Oscillation on South America. Nature Reviews Earth & Environment, v. 1, 215-231. https://doi.org/10.1038/s43017-020-0040-3

Centro de Previsão de Tempo e Estudos Climáticos, 2023. El Niño e La Niña (Accessed August 28, 2023). at: http://enos.cptec.inpe.br.

Chavda, D.; Li, J.; Farahmand, A., 2024. Assessing the influence of El Niño on the California precipitation regime during the satellite precipitation era. Hydrological Processes, v. 38 (5), e15160. https://doi.org/10.1002/hyp.15160

Chen, S.; Zhang, L.; Zhang, Y.; Guo, M.; Liu, X., 2020. Evaluation of Tropical Rainfall Measuring Mission (TRMM) satellite precipitation products for drought monitoring over the middle and lower reaches of the Yangtze River Basin, China. Journal of Geographical Sciences, v. 30, 53-67. https://doi.org/10.1007/s11442-020-1714-y

Collischonn, B.; Allasia, D.; Collischonn, W.; Tucci, C.E.M., 2007. Desempenho do satélite TRMM na estimativa de precipitação sobre a bacia do Paraguai superior. Revista Brasileira de Cartografia, v. 59 (1), 93-99. https://doi.org/10.14393/rbcv59n1-43965

Duarte, M.L.; Ribeiro, A., 2023. Influência do El Niño e La Niña na produtividade de plantios de Eucalipto em distintas regiões no Brasil. Ciência Florestal, v. 33 (1), e61334. https://doi.org/10.5902/1980509861334

Fan, N.; Lin, X.; Guo, H, 2023. An analysis for the applicability of global precipitation measurement mission (GPM) IMERG precipitation data in typhoons. Atmosphere, v. 14 (8), 1224. https://doi.org/10.3390/atmos14081224

Fan, Z.; Li, W.; Jiang, Q.; Sun, W.; Wen, J.; Gao, J., 2021. A comparative study of four merging approaches for regional precipitation estimation. IEEE Access, v. 9, 33625-33637. https://doi.org/10.1109/ACCESS.2021.3057057

Glantz, M.H.; Ramirez, I.J., 2020. Reviewing the Oceanic Niño Index (ONI) to enhance societal readiness for El Niño's impacts. International Journal of Disaster Risk Science, v. 11, 394-403. https://doi.org/10.1007/s13753-020-00275-w

Guo, R.; Fan, X.; Zhou, H.; Liu, Y., 2024. Multi-sensor precipitation estimation from space: data sources, methods and validation. Remote Sensing, v. 16 (24), 4753. https://doi.org/10.3390/rs16244753

Haines, A.; Lam, H. C., 2023. El Niño and health in an era of unprecedented climate change. The Lancet, v. 402 (10415), 1811-1813. https://doi.org/10.1016/S0140-6736(23)01664-1

Huffman, G.J.; Adler, R.F.; Bolvin, D.T.; Gu, G.; Nelkin, E.J.; Bowman, K.P.; Wolff, D.B., 2007. The TRMM Multisatellite Precipitation Analysis (TMPA): Quasi-global, multiyear, combined-sensor precipitation estimates at fine scales. Journal of Hydrometeorology, v. 8 (1), 38-55. https://doi.org/10.1175/JHM560.1

Instituto de Pesquisa Econômica Aplicada (IPEA), 2021. Região Sudeste: Diagnóstico e perspectivas – Cadernos de Desenvolvimento Regional. Instituto de Pesquisa Econômica Aplicada, Brasília (Accessed August 11, 2025) at:. https://www.ipea.gov.br/portal/images/stories/PDFs/livros/livros/210223_cadernos_regiao_sudeste.pdf

Koralegedara, S.B.; Huang, W.R.; Tung, P.H.; Chiang, T.Y., 2023. El Niño-Southern Oscillation modulation of springtime diurnal rainfall over a tropical Indian Ocean island. Earth and Space Science, v. 10 (5), e2023EA002832. https://doi.org/10.1029/2023EA002832

Kukulies, J.; Chen, D.; Wang, M., 2020. Temporal and spatial variations of convection, clouds and precipitation over the Tibetan Plateau from recent satellite observations. Part II: Precipitation climatology derived from global precipitation measurement mission. International Journal of Climatology, v. 40 (11), 4858-4875. https://doi.org/10.1002/joc.6493

Kummerow, C.; Simpson, J.; Thiele, O.; Barnes, W.; Chang, A.S.; Adler, R.; Olson, W.S., 2000. The status of the tropical rainfall measuring mission (TRMM) after two years in orbit. Journal of Applied Meteorology, v. 39 (12), 1965-1982. https://doi.org/10.1175/1520-0450(2001)040<1965:TSOTTR>2.0.CO;2

Lal, D.; Singh, S., 2023. Impact of El-Nino and La-Nina episodes on rainfall variability and crop yield. International Journal of Environment and Climate Change, v. 13 (10), 2046-2051. https://doi.org/10.9734/IJECC/2023/v13i102865

Lee, J.H.; Julien, P.Y.; Cho, J.; Lee, S.; Kim, J.; Kang, W., 2023. Rainfall erosivity variability over the United States associated with large-scale climate variations by El Niño/southern oscillation. Catena, v. 226, 107050. https://doi.org/10.1016/j.catena.2023.107050

Li, Y.; Yi, F.; Wang, Y.; Gudaj, R., 2019. The Value of El Niño-Southern oscillation forecasts to China's agriculture. Sustainability, v. 11 (15), 4184. https://doi.org/10.3390/su11154184

Louzada, F.L.D.O.; Xavier, A.C.; Pezzopane, J.E., 2018. Climatological water balance with data estimated by tropical rainfall measuring mission for the Doce river basin. Engenharia Agrícola, v. 38 (3), 376-386. https://doi.org/10.1590/1809-4430-Eng.Agric.v38n3p376-386/2018

Ma, Y.; Tang, G.; Long, D.; Yong, B.; Zhong, L.; Wan, W.; Hong, Y., 2016. Similarity and error intercomparison of the GPM and its predecessor-TRMM multisatellite precipitation analysis using the best available hourly gauge network over the Tibetan Plateau. Remote Sensing, v. 8 (7), 569. https://doi.org/10.3390/rs8070569

Macharia, J.M.; Ngetich, F.K.; Shisanya, C.A., 2020. Comparison of satellite remote sensing derived precipitation estimates and observed data in Kenya. Agricultural and Forest Meteorology, v. 284, 107875. https://doi.org/10.1016/j.agrformet.2019.107875

Medeiros, S.A.; Nóbrega, R.A.; Moraes Neto, J.M.; Barreto, B.B.; Vasconcelos, G.N.; Diniz, R.R.S., 2020. Investigação da influência do El Niño e da La Niña sobre a variabilidade da precipitação na cidade de Patos, Paraíba. Revista Brasileira de Geografia Física, v. 13 (1), 336-349. https://doi.org/10.26848/rbgf.v13.1.p336-349

Mekonnen, K.; Melesse, A.M.; Woldesenbet, T.A., 2021. Spatial evaluation of satellite-retrieved extreme rainfall rates in the Upper Awash River Basin, Ethiopia. Atmospheric Research, v. 249, 105297. https://doi.org/10.1016/j.atmosres.2020.105297

Mokhov, I.I., 2022. Changes in the frequency of phase transitions of different types of El Niño phenomena in recent decades. Izvestiya, Atmospheric and Oceanic Physics, v. 58 (1), 1-6. https://doi.org/10.1134/S000143382201008X

Montazeri, M.; Kiany, M.S.K.; Masoodian, S.A., 2020. Evaluation of Tropical Rainfall Measuring Mission (TRMM) Multi-satellite Precipitation Analysis (TMPA v7) in drought monitoring over southwest Iran. Climate Research, v. 82, 55-73. https://doi.org/10.3354/cr01622

Nan, L.; Yang, M.; Wang, H.; Xiang, Z.; Hao, S., 2021. Comprehensive evaluation of global precipitation measurement mission (GPM) IMERG precipitation products over Mainland China. Water, v. 13 (23), 3381. https://doi.org/10.3390/w13233381

Pedreira Junior, A.L.; Querino, C.A.S.; Biudes, M.S.; Machado, N.G.; Santos, L.O.F.D.; Ivo, I.O., 2020. Influence of El Niño and La Niña phenomena on seasonality of the relative frequency of rainfall in southern Amazonas mesoregion. Revista Brasileira de Recursos Hídricos, v. 25, e24. https://doi.org/10.1590/2318-0331.252020190152

Raj, A.D.; Sooryamol, K.R.; Raj, A.D., 2021. Exploring temporal rainfall variability and trends over a tropical region using tropical rainfall measurement mission (TRMM) and observatory data. Hydrospatial Analysis, v. 5 (2), 56-71. https://doi.org/10.21523/gcj3.2021050202

Reboita, M.S.; Oliveira, K.R.; Corrêa, P.Y.C.; Rodrigues, R., 2021. Influência dos diferentes tipos do fenômeno El Niño na precipitação da América do Sul. Revista Brasileira de Geografia Física, v. 14 (2), 729-742. https://doi.org/10.26848/rbgf.v14.2.p729-742

Restrepo-Coupe, N.; Campos, K.S.; Alves, L.F.; Longo, M.; Wiedemann, K.T.; Oliveira, R.C.; Aragão, L.E.O.C.; Christoffersen, B.O.; Camargo, P.B.; Figueira, A.M.S.; Ferreira, M.L.; Oliveira, R.S.; Penha, D.; Prohaska, N.; Araujo, A.C.; Daube, B.C.; Wofsy, S.C.; Saleska, S.R., 2024. Contrasting carbon cycle responses to dry (2015 El Niño) and wet (2008 La Niña) extreme events at an Amazon tropical forest. Agricultural and Forest Meteorology, v. 353, 110037. https://doi.org/10.1016/j.agrformet.2024.110037

Retalis, A.; Katsanos, D.; Tymvios, F.; Michaelides, S., 2020. Comparison of GPM IMERG and TRMM 3B43 Products over Cyprus. Remote Sensing, v. 12 (19), 3212. https://doi.org/10.3390/rs12193212

Santos, P.H.N.; Ferreira, W.S.; Santana, B.L.P., 2023. Repercussões do El Niño e La Niña na precipitação do estado de Sergipe – Brasil. Revista Brasileira de Climatologia, v. 33 (19), 409-437. https://doi.org/10.55761/abclima.v33i19.17395

Sharma, S.; Chen, Y.; Zhou, X.; Yang, K.; Li, X.; Niu, X.; Hu, X.; Khadka, N., 2020. Evaluation of GPM-Era satellite precipitation products on the southern slopes of the Central Himalayas against rain gauge data. Remote Sensing, v. 12 (11), 1836. https://doi.org/10.3390/rs12111836

Silva, A.S.A.; Stosic, B.; Menezes, R.S.C.; Singh, V.P., 2019. Comparison of interpolation methods for spatial distribution of monthly precipitation in the state of Pernambuco, Brazil. Journal of Hydrologic Engineering, v. 24 (3), 04018068. https://doi.org/10.1061/(ASCE)HE.1943-5584.0001743

Silva, K.A.; Rolim, G.S.; Valeriano, T.T.B.; Moraes, J.R.S.C., 2020. Influence of El Niño and La Niña on coffee yield in the main coffee-producing regions of Brazil. Theoretical and Applied Climatology, v.139, 1019-1029. https://doi.org/10.1007/s00704-019-03039-9

Suroso, S.; Santoso, P.B.; Birkinshaw, S.; Kilsby, C.; Bárdossy, A.; Aldrian, E., 2023. Assessment of TRMM rainfall data for flood modelling in three contrasting catchments in Java, Indonesia. Journal of Hydroinformatics, v. 25 (3), 797-814. https://doi.org/10.2166/hydro.2023.132

Tan, M.L.; Duan, Z., 2017. Assessment of GPM and TRMM precipitation products over Singapore. Remote Sensing, v. 9 (7), 720. https://doi.org/10.3390/rs9070720

Tunas, I.G.; Herman, R.K.; Arafat, Y., 2024. Application of tropical rainfall measuring mission (TRMM) data for flood estimation in lack data catchment. IOP Conference Series: Earth and Environmental Science, v.1343, 012003. https://doi.org/10.1088/1755-1315/1343/1/012003

Woods, D.; Kirstetter, P.E.; Vergara, H.; Duarte, J.A.; Basara, J., 2023. Hydrologic evaluation of the global precipitation measurement mission over the US: Flood peak discharge and duration. Journal of Hydrology, v. 617 (Part C), 129124. https://doi.org/10.1016/j.jhydrol.2023.129124

Wu, D., 2024. History, mechanisms, and future directions of the El Niño-Southern oscillation under the severe climate change. Highlights in Science, Engineering and Technology, v. 88, 681-686. https://doi.org/10.54097/d1b2sb32

Yang, Y.; Tang, G.; Lei, X.; Hong, Y.; Yang, N., 2018. Can satellite precipitation products estimate probable maximum precipitation: A comparative investigation with gauge data in the Dadu River basin. Remote Sensing, v. 10 (1), 41. https://doi.org/10.3390/rs10010041

Zhao, Y.; Liu, Q.; Chen, L., 2023. Evaluation of GPM and TRMM and their capabilities for capturing solid and light precipitations in the headwater basin of the Heihe River. Atmosphere, v. 14 (3), 453. https://doi.org/10.3390/atmos14030453

Zhang, C.; Chen, X.; Shao, H.; Chen, S.; Liu, T.; Chen, C.; Ding, Q.; Du, H., 2018. Evaluation and intercomparison of high-resolution satellite precipitation estimates – GPM, TRMM, and CMORPH in the Tianshan Mountain Area. Remote Sensing, v. 10 (10), 1543. https://doi.org/10.3390/rs10101543